PHYSICAL REVIEW B **81**, 041407(R) (2010)

Model for transient elongation and drift of islands on vicinal substrates

M. Dufay and O. Pierre-Louis

Laboratoire de Physique de la Matière Condensée et Nanostructures, Université Lyon 1, 43 Boulevard 11 Novembre 1918, F69622 Villeurbanne, France; Rudolf Peierls Centre for Theoretical Physics, Oxford University, 1 Keble Road, OX1 3NP Oxford, United Kingdom; Laboratoire de Spectrométrie Physique, Université Joseph Fourier, 140 Avenue de la Physique, 38402 Saint Martin D'Hères, France

(Received 27 November 2009; published 8 January 2010)

During their relaxation to equilibrium, crystalline islands on misoriented (vicinal) substrates drift and deform. Our model indicates a generic and transient elongation perpendicular to the drift direction. The maximum elongation and the drift exhibit distinctive behaviors depending on the dominant energy contribution (interfacial energy, wetting potential, or elastic energy) and the dominant mass transport process (diffusion or attachment-detachment).

DOI: 10.1103/PhysRevB.81.041407 PACS number(s): 81.10.Aj, 05.70.Ln, 68.55.−a

Solid films, deposited on crystal surfaces by means of various epitaxial growth techniques, exhibit a wide range of shapes ranging from atomically flat films to scattered islands. The morphology obtained from the growth process may be stable or may undergo some instability, such as reshaping of the islands[1] or dewetting of films.[2–4] This complex postdeposition dynamics is driven by the reduction of the adsorbate free energy. Nevertheless, the precise evolution of the system crucially depends on mass transport processes. A major limiting effect in the kinetics of shape relaxation is the nucleation barrier for the formation of new atomic layers on a facet.[5–8] Because of the large times needed to overcome this barrier, islands often cannot retrieve their equilibrium height when their top is facetted. However, a small misorientation of the substrate with respect to the top facet—i.e., a vicinal substrate—allows for a different pathway to reach equilibrium. A change in the island height is indeed obtained from a drift of the island. Such a spontaneous drift associated with a nucleationless shape relaxation was recently discovered in dewetting experiments.[9] Since most wafers exhibit spurious misorientations due to imperfections in the growth and cleaning processes, the drift is expected to be a generic feature and should be observed on a wide variety of surfaces. Moreover, such a drift may be used to transport mass at the surface, so as to obtain controlled island positioning on patterned substrates.[10]

In this Rapid Communication, we show that island relaxation exhibits distinctive behaviors depending on the dominant driving force (interface energy, wetting potential, or elastic energy) and the dominant mass transport process (diffusion or attachment-detachment). Moreover, we report on some unexpected behavior. (i) When the system is driven by interfacial energy or by a monotonically decaying wetting potential, islands exhibit a transient elongation perpendicular to the drift, in agreement with experiments.[9] (ii) When the elastic energy dominates, a much stronger—but still transient—elongation results from a well-known shape transition first identified by Tersoff and Tromp.[1] An elongation perpendicular to the drift is dynamically favored. (iii) When mass transport is limited by diffusion, the drift velocity is independent of the island volume.

Schematics of the model are presented in Fig. 1. The island is rectangular, and the vicinal substrate is misoriented with a small angle θ. In the following, we shall neglect contributions $\sim\theta^2$. Nucleation of new layers on the top facet is absent, due to the existence of a nucleation barrier,[5,6] and the sides behave as rough surfaces. Such a model mimics the islands observed in Ref. 9 and aims to describe more generally flat islands with a top facet. Choosing the origin of the x axis at the intersection between the top facet plane and the substrate, the local height of the island along z reads $h(x)=x\tan(\theta)$. The positions of the upper and lower sides are denoted as x_U and x_D and that of the lateral sides are y_+ and y_-. The average island position $\mathcal{X}=(x_U+x_D)/2$, and the average height $\mathcal{H}$ are related to the island volume V via $\mathcal{H}=\mathcal{X}\tan(\theta)=V/(l_T l_\perp)$, where $l_T=x_D-x_U$ and $l_\perp=y_+-y_-$.

We assume that the film edge of height h_* is circular, with a large radius $R_* \gg h_*, l_T, l_\perp, \mathcal{X}$, so that the island is always approximately in the center of the denuded zone, as in Fig. 1. Global mass conservation imposes $\pi R_*^2 h_* = V$.

Mass conservation at the island edge positions $\xi_i = x_U, x_D, y_+, y_-$ reads $d\xi_i/dt = J_i/(dV/\Omega d\xi_i)$, where Ω is the atomic volume. The total mass flux arriving on side $i=U,D,+,-$ is $J_i = J_i^< + J_i^>$, where $J_i^<$ and $J_i^>$ indicate the fluxes coming from island top facet and from the substrate, respectively. A simple ansatz is designed for diffusion-limited transport,

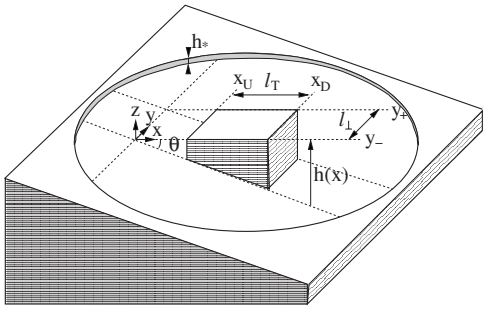

FIG. 1. A rectangular island on a vicinal substrate. In the first stage, the island grows by mass transfer from the film of thickness h_* and a denuded zone surrounds the island. In the second stage, the initial film has disappeared by mass transfer to the islands.

 ©2010 The American Physical Society

$$J_i^\nu = L_i \frac{D^\nu c_{eq}^\nu}{k_B T d_i^\nu}(\mu^\nu - \mu_i), \tag{1}$$

where ν is $>$ or $<$. For each side i of length L_i, the distance to the center of the top facet is $d_i^<$. We have defined the diffusion constant and the equilibrium concentration of mobile atoms on the island facet $D^<$ and $c_{eq}^<$ and on the bare substrate $D^>$ and $c_{eq}^>$. The chemical potentials of the sides are defined as $\mu_i=(dE/d\xi_i)/(dV/\Omega d\xi_i)$, where E is the total island energy. The chemical potential on the top facet $\mu^<$ is fixed by the mass conservation relation $\Sigma_i J_i^<=0$.

We decompose the diffusion field on the bare substrate between the island and the film edges in two zones, depending on the distance d to the center of the island: zone I, where $d<R^>$, and zone II, where $R^><d<R_*$. In the junction between the two zones, at $d=R^>$, the chemical potential is $\mu^>$. In zone I, mass transport is modeled via Eq. (1) with the diffusion length $d_i^>=R^>-d_i^<$. In zone II, we assume that the adatom concentration is axisymmetric and only depends on d. Solving the diffusion equation for the adatom concentration in zone II, the total mass flux from the film edge is found to be

$$J^> = \frac{2\pi D^> c_{eq}^>}{k_B T \ln[R_*/R^>]}(\mu_* - \mu^>), \tag{2}$$

where $\mu_*=\Omega(-\gamma_S/R_*+\gamma_T/h_*)$ is the film edge chemical potential. Mass conservation in the depletion zone $\Sigma_i J_i^>=J^>$ fixes $\mu^>$. Finally, we use a simple ansatz: $R^>=x(l_T+l_\perp)$. Comparing the full numerical solution of the diffusion field around a rectangle with our model, the best fit is obtained for $x\approx 3/4$.

We consider a total free energy $E=E_I+E_E$, where E_E is an elastic energy. We shall first discard E_E and consider a free energy contribution of the form

$$E_I = \gamma_S(h_U + h_D)(l_\perp + l_T) + \mathcal{V}[x_U,x_D] l_T l_\perp, \tag{3}$$

where $h_U=h(x_U)$, $h_D=h(x_D)$, and γ_S is the surface free energy on the sides. Moreover,

$$\mathcal{V}[x_U,x_D] = \gamma_T + \frac{1}{l_T}\int_{x_U}^{x_D} dx \mathcal{W}[h(x)], \tag{4}$$

with $\gamma_T=\gamma_{top}+(\gamma_{int}-\gamma_{sub})/\cos\theta$, where γ_{top}, γ_{int}, and γ_{sub} are the free energies of the top facet, the island substrate, and the bare substrate, respectively. Finally, $\mathcal{W}[h]$ is a wetting potential which may account, e.g., for elastic coupling of the surface and interface stresses,[11] electronic energies,[12] or the van der Waals energy.[13]

The model dynamics is then composed of two main stages. First, the island grows by mass transfer from the film. Second, the initial film has completely disappeared, and the island drifts downhill without (or with very slow) change of the total volume.

Let us start with the growth stage. When $\phi<1$, with $\phi=D^< c_{eq}^</(D^> c_{eq}^>)$, there is no drift, and x_U tends to a constant. The aspect ratio converges to a constant r_{sat}, obeying

$$2\phi \frac{r_{sat}(1-2\eta)-1}{(r_{sat}+1)(1+2\eta+f)} = \frac{4\eta-1}{(r_{sat}+2)(1+\eta)}, \tag{5}$$

with $f=f(x,r)=2r/[2x(r+1)-1]$ and $\eta=f(x,1/r)/f(x,r)$. We find $r_{sat}\approx 9.4$ for $\phi\to 0$, monotonously decreasing to $r_{sat}\approx 5$ for large ϕ. From an asymptotic analysis of Eq. (2), we also obtain that $V\sim t$ up to logarithmic corrections. In addition $V\approx r_{sat} l_T^3 \tan\theta/2$, so that $l_T\sim l_\perp\sim t^{1/3}$.

When $\phi>1$, r also reaches a constant value, approximately given by Eq. (5), but x_U is not constant anymore and the island drifts. Experiments[9] indicate that the island drifts in the growth stage, showing that $\phi>1$. Note that, when $\phi\to\infty$, the model is not consistent anymore because the depletion zone radius R_* is not much larger than the drift-induced island displacement $\mathcal{X}$.

However, the asymptotic behavior is not necessarily reached in experiments. Using typical orders of magnitude for Cu islands on Ru substrates,[9] $\theta=3.4\times10^{-3}$, $\Omega=12$ Å^3, and $h_*=2.1$ Å, we choose $D^> c_{eq}^>=1.1\times10^5$ s^{-1} so that the numerical solution of our model provides the observed maximum island volume at $t=10$ min. With these parameters, the aspect ratio increases up to $r\approx 2.8<r_{sat}$, in good agreement with the observed maximum aspect ratio at 10 min: $r=2.6$.[9] The result depends weakly on γ_T/γ_S and ϕ.

Once the initial film has disappeared by mass transfer to the islands, we reach the second stage of the dynamics. We neglect mass exchange between different islands, which leads to a slow Ostwald ripening process, and focus on the consequences of mass transport on one island. In this regime, $J_i^>$ vanish and V is conserved. We obtain two dynamical regimes: fast relaxation at constant position $\mathcal{X}$ and fast relaxation at constant $l_\perp$ when $l_\perp \gg l_T$ or $x_U\to 0$.

The numerical solution of the full model, shown on Fig. 2(a) for $\mathcal{W}[h]=0$, clearly indicates the two expected regimes. As a consequence, the dynamics of an island with initial aspect ratio $r_{init}\sim 1$ is composed of three phases. First, a decrease of l_T at constant $l_\perp$ leads to an increasing aspect ratio $r=l_\perp/l_T$ up to a maximum $r_{\max}^I$. Second, a relaxation at almost constant $\mathcal{X}$ leads to the decrease of r. Third, the island drifts slowly, while $r\approx 1$. The drift stops when the island reaches its equilibrium height.

In the limit where the island is far from its initial position $\mathcal{X}\gg l_T$, which implies $\mathcal{V}[x_U,x_D]\approx\gamma_T+\mathcal{W}[\mathcal{H}]$, and for an initial aspect ratio $r=r_{init}$, we find

$$r_{\max}^I \approx \left(\frac{\bar{\mathcal{V}}[\mathcal{H}_{\max}]}{2\gamma_S \tan\theta}\right)^{1/4} r_{init}^{3/2}, \tag{6}$$

where $\bar{\mathcal{V}}[\mathcal{H}]=\gamma_T+\mathcal{W}[\mathcal{H}]-\mathcal{H}\mathcal{W}'[\mathcal{H}]$ and $\mathcal{H}_{\max}=V^{1/3} r_{\max}^I (\tan\theta/2)^{2/3}/r_{init}^{4/3}$. A quantitative analysis of Eq. (6) is delicate because we do not know r_{init}. Indeed, the experimental initial condition corresponds to the result of the growth stage discussed earlier.

We shall now analyze the drift velocity, focusing on the limit where the island is flat and far from its equilibrium shape, i.e., $l_T, l_\perp \gg 2\mathcal{H}\gamma_S/\bar{\mathcal{V}}[\mathcal{H}]$. Then, an expansion for $\mathcal{X}\gg l_T$ provides us with the drift velocity

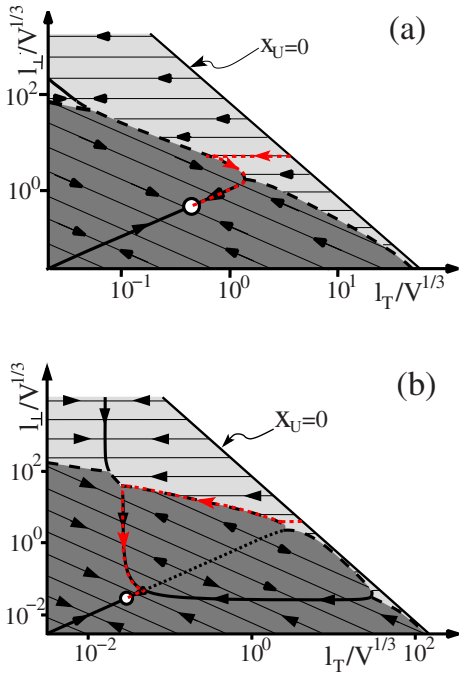

FIG. 2. (Color online) Dynamical flow of an island on a vicinal substrate from the solution of the full model with conserved volume V. Lines are obtained from the divergence of the normalized velocity. Possible configurations are the shaded area to the left of the line $x_U=0$. The dark gray area corresponds to the regime of fast relaxation at constant $\mathcal{X}$ and the light gray to fast relaxation at constant l_T. Arrows indicate the direction of the evolution, and a white dot corresponds to the equilibrium configuration. Thick solid lines indicate the slow dynamics. Model parameters: $\theta=\pi/100$. (a) Interface energy with $\mathcal{W}[h]=0$, $\gamma_T/\gamma_S=0.063$; (b) elastic energy, with $V^{1/3}/d_0=10^{2.5}$. A bifurcation leads to two branches with slow dynamics. The dotted line indicates an unstable line.

$$\partial_t \mathcal{X} = \frac{\Omega^2 D^< c_{eq}^<}{k_B T} \frac{\bar{\mathcal{V}}[\mathcal{H}]}{\mathcal{X}^3 \tan^2(\theta)}, \tag{7}$$

which is independent of V. This leads to $\mathcal{X}\sim t^{1/4}$ when $\mathcal{W}[\mathcal{H}]\ll\gamma_T$, in agreement with the scaling proposed in Ref. 9. In experiments, $\mathcal{H}\approx 53$ monolayers after 100 min. Using Eq. (7) with the numerical value $D^> c_{eq}^> = 1.1\times 10^5$ s^{-1} extracted above and a typical value $\gamma_T \approx 1$ J m^{-2}, we obtain $\phi\approx 40$ (i.e., $D^< c_{eq}^< = 4\times 10^6$ s^{-1}). Such a result is in qualitative agreement with the previous statement $\phi>1$ obtained from the existence of a drift in the growth stage.

In contrast, the driving force may be dominated by the wetting potential $\mathcal{W}[\mathcal{H}]\gg\gamma_T$. Assuming $\mathcal{W}[\mathcal{H}]\sim\mathcal{H}^{-\beta}$ leads to a different scaling behavior $\mathcal{X}\sim t^{1/(\beta+4)}$. The exponent β depends on the physical origin of the wetting potential: $\beta=2$ for van der Waals forces[13] or $\beta=1$ for surface-interface stress coupling.[11] In the presence of an oscillatory wetting potential caused by electron confinement,[12] the island could stop in a state with $\bar{\mathcal{V}}[\mathcal{H}]=0$.[21]

Let us now consider the elastic energy induced by the lattice mismatch between the island and the substrate. Here, we focus on the second stage of the dynamics, where mass transport essentially occurs on the island. In the limit where the island is flat (i.e., $\mathcal{H}\ll l_T, l_\perp$) and in the absence of dislocations, we may follow the approximation in Ref. 1. The total surface force density $\mathbf{f}(\mathbf{r})$ is the sum of a surface force density $\alpha\tan\theta$ at the interface under the island and of four linear force densities $\alpha h(x)$ along the sides. The total elastic energy reads

$$E_E = \frac{1}{2}\int \mathbf{dr}\int \mathbf{dr}'\mathcal{G}_{j,k}(\mathbf{r}-\mathbf{r}')\mathbf{f}_j(\mathbf{r})\mathbf{f}_k(\mathbf{r}'), \tag{8}$$

where $\mathbf{r},\mathbf{r}'$ are two-dimensional vectors in the x,y plane and $\mathcal{G}_{j,k}$ is the surface elastic Green's function.[14,15] We assume that $\theta\ll 1$ and $\mathcal{G}_{j,k}$ is calculated as if the substrate was along the x,y plane. We introduce a cutoff d_0 in Eq. (8), which can be related to observable quantities such as a formation length[16–18] or the width of the sides.[1]

The energy E_E exhibits a minimum at $x_U=0$ when $V<V_c\approx 390 d_0^3\tan(\theta)$. For $V>V_c$, the minimum is at $x_U>0$, and a drift is expected. Figure 2(b) shows the dynamical flow of the island when $V>V_c$. For the same reason as in the interfacial energy driven evolution, the downhill drift is first accompanied by an elongation perpendicular to the drift. But after this initial dynamics, the islands exhibit a much larger elongation, which can be traced back to the shape instability for islands with fixed height identified by Tersoff and Tromp.[1] These authors indeed found that while the equilibrium shape of small islands is a square, large islands exhibit an elongated equilibrium shape. Note that an elongation along y is favored by the initial dynamics with $r\sim 1$.

The maximum aspect ratio is obtained in the limit $\mathcal{X}\gg l_T$ and $l_\perp\gg l_T$ as

$$r_{\max}^E = C V^{1/2}\tan(\theta)^{-1/2} d_0^{-3/2} e^{-3(3+\sigma)/8(1-\sigma)}, \tag{9}$$

where $C\approx 0.175$ and $\sigma\approx 0.3$ is the Poisson ratio. In contrast to Eq. (6), we now find that $r_{\max}^E$ does not depend on the initial aspect ratio.

A typical value of d_0 can be extracted from experiments. In order to do so, we consider an elongated rectangular island of lateral lengths λ and Λ, with $\lambda\ll\Lambda$ and $\theta\to 0$. Energy minimization at fixed V and $\mathcal{X}$ (or $\mathcal{H}$) leads to $\lambda = 2d_0\exp[1/(1-\sigma)]$, and

$$E_E|_{\mathcal{H},V} = \frac{\alpha^2(1-\sigma^2)}{\pi Y d_0}\mathcal{H} V e^{-1/(1-\sigma)}, \tag{10}$$

where Y is the substrate Young modulus. Comparing λ to the width of elongated islands of $CoSi_2/Si(100)$,[19] we find $d_0\approx 8$ nm. From Eq. (9), on a vicinal surface with $\theta=0.01$ with a typical volume $V=10^6$ nm^3,[19] we find $r_{\max}^E\approx 13$ for $CoSi_2/Si(100)$.

After the maximum aspect ratio has been reached, the elongated island exhibits a slow drift. The energy [Eq. (10)] of an elongated island behaves as if it was derived from a wetting potential $\mathcal{W}[\mathcal{H}]\sim\mathcal{H}^2$ and $\gamma_T=0$. Thus, we may use Eq. (7), leading to

$$\partial_t \mathcal{X} = \frac{\Omega^2 D c_{eq}}{k_B T} \frac{\alpha^2(1-\sigma^2)}{\pi Y d_0} e^{-1/(1-\sigma)} \frac{1}{\mathcal{X}}, \tag{11}$$

so that $\mathcal{X} \sim t^{1/2}$. Surprisingly, the drift evolution equation for $\mathcal{X}$ is independent of θ and V. Furthermore, Eq. (11) is independent of the elongation direction.

Finally, elongated islands transform into compact islands (square up to small corrections $\sim\theta^2$) at long times. Compact islands are obtained for $\mathcal{H} d_0^2 \geq V(3-2^{3/2}) e^{-2^{3/2}-2\sigma/(1-\sigma)}$. Hence, the bifurcation from elongated to compact, found by decreasing V at constant $\mathcal{H}$ in Ref. 1, is obtained during the drift on vicinal surfaces by increasing the height $\mathcal{H}$ at constant V.

The results of the diffusion-limited dynamics presented above can be translated to the case of attachment limited dynamics. The attachment-detachment regime is obtained upon the substitution[20] $D^\nu / d^\nu \to \kappa^\nu$ in Eq. (1), where κ^ν is independent of the island geometry, and a similar law replaces Eq. (2). However, a detailed analysis would be lengthy, and we shall therefore present the main results, focusing on the drift regime where V is conserved. Our main result is that the dynamics is not qualitatively affected, and dynamical diagrams are similar to those of Fig. 2. Nevertheless, different scalings are obtained and the drift velocity now depends on V.

We first consider the energy E_I in the absence of wetting potential, i.e., $\mathcal{W}[h]=0$. We find an elongation up to $r^I_{\max} = (\gamma_T / 2\gamma_S \tan\theta)^{1/5} r_{init}^{6/5}$, followed by a drift with

$$\partial_t \mathcal{X} = \kappa^< c_{eq} V^{1/2} \gamma_T / [2 \tan(\theta)^{5/2} \mathcal{X}^{7/2} k_B T]. \tag{12}$$

This leads to $\mathcal{X} \sim t^{2/9}$, which could be difficult to distinguish from the $t^{1/4}$ obtained in the diffusion-limited regime. An easier way to identify the limiting mass transport process would be to check how the island velocity varies with the volume.

In the case where the elastic energy E_E dominates and for $V > V_c$, the scalings depend on the direction of the elongation. If $r > 1$, we find $r^E_{\max} \sim (2V/\tan\theta)^{2/3}/d_0^2$ and a subsequent scaling $\partial_t \mathcal{X} \sim \mathcal{X}^{-1}$. In contrast, when $r < 1$, we find a minimum aspect ratio $r^E_{\min} \sim (\tan\theta/2V)^{3/2} d_0^{3/2}$ and $\partial_t \mathcal{X} \sim \mathcal{X}^{-2}$.

As a conclusion, we have studied the shape changes and drift of islands on misoriented substrates. Island elongation and velocity exhibit distinctive behaviors, depending on the dominant energy contribution and mass transport process.

The authors acknowledge support from ANR-PNANO grants Nanomorphogénèse and DéFiS and wish to thank the kind hospitality of J. Yeomans in Oxford.

[1] J. Tersoff and R. M. Tromp, Phys. Rev. Lett. **70**, 2782 (1993).
[2] K. Thürmer and N. C. Bartelt, Phys. Rev. Lett. **100**, 186101 (2008).
[3] O. Pierre-Louis, A. Chame, and Y. Saito, Phys. Rev. Lett. **99**, 136101 (2007).
[4] B. Yang, P. Zhang, D. E. Savage, M. G. Lagally, G. H. Lu, M. Huang, and F. Liu, Phys. Rev. B **72**, 235413 (2005).
[5] W. W. Mullins and G. S. Rohrer, J. Am. Ceram. Soc. **83**, 214 (2000).
[6] N. Combe, P. Jensen, and A. Pimpinelli, Phys. Rev. Lett. **85**, 110 (2000).
[7] K. Thürmer, J. E. Reutt-Robey, and E. D. Williams, Surf. Sci. **537**, 123 (2003).
[8] G. S. Rohrer, C. L. Rohrer, and W. W. Mullins, J. Am. Ceram. Soc. **84**, 2099 (2001).
[9] W. Ling *et al.*, Surf. Sci. Lett. **570**, L297 (2004).
[10] K. F. McCarty, Nano Lett. **6**, 858 (2006).
[11] K. McCarty *et al.*, New J. Phys. **11**, 043001 (2009).
[12] Z. Zhang, Q. Niu, and C.-K. Shih, Phys. Rev. Lett. **80**, 5381 (1998).
[13] Z. Suo and Z. Zhang, Phys. Rev. B **58**, 5116 (1998).
[14] L. D. Landau and E. M. Lifshitz, *Theory of Elasticity* (Pergamon Press, New York, 1970).
[15] B. Houchmandzadeh and C. Misbah, J. Phys. I **5**, 685 (1995).
[16] J. B. Hannon, J. Tersoff, and R. M. Tromp, Science **295**, 299 (2002).
[17] N. V. Medhekar, V. B. Shenoy, J. B. Hannon, and R. M. Tromp, Phys. Rev. Lett. **99**, 156102 (2007).
[18] V. I. Marchenko, Sov. Phys. JETP **54**, 605 (1981).
[19] S. H. Brongersma, M. R. Castell, D. D. Perovic, and M. Zinke-Allmang, Phys. Rev. Lett. **80**, 3795 (1998).
[20] S. V. Khare, N. C. Bartelt, and T. L. Einstein, Phys. Rev. Lett. **75**, 2148 (1995).
[21] Note that, due to the fixed volume constraint, this height does not correspond to a local minima of $\mathcal{W}[\mathcal{H}]$, which would be solution of $\mathcal{W}'[\mathcal{H}]=0$.